Original Article

L-carnitine affects osteoblast differentiation in NIH3T3 fibroblasts by the IGF-1/PI3K/Akt signalling pathway

Pinglan Ge[1,2], Yazhou Cui[1], Fang Liu[1,2], Jing Luan[1], Xiaoyan Zhou[1], Jinxiang Han[1,*]

[1] *Key Laboratory for Rare Disease Research of Shandong Province, Key Laboratory for Biotech Drugs of the Ministry of Health, Shandong Medical Biotechnological Center, Shandong Academy of Medical Sciences, Ji'nan, Shandong, China;*
[2] *School of Medicine and Life Sciences, University of Jinan-Shandong Academy of Medical Science, Ji'nan, Shandong, China.*

Summary	**Fibroblasts in soft tissues are one of the progenitors of ectopic calcification. Our previous experiment found that the serum concentrations of small metabolite L-carnitine (LC) decreased in an ectopic calcification animal model, indicating LC is a potential calcification or mineralization inhibitor. In this study, we investigated the effect of LC on NIH3T3 fibroblast osteoblast differentiation, and explored its possible molecular mechanisms. Two concentrations of LC (10 µM and 100 µM) were added in Pi-induced NIH3T3 fibroblasts, cell proliferation was compared by MTT assays, osteoblast differentiation was evaluated by ALP activity, mineralized nodules formation, calcium deposition, and expressions of the osteogenic marker genes. Our results indicated that 10 µM LC increased the proliferation of NIH3T3 cells, but 100 µM LC slightly inhibited cell proliferation. 100 µM LC inhibits NIH3T3 differentiation as evidenced by decreases in ALP activity, mineralized nodule formation, calcium deposition, and down-regulation of the osteogenic marker genes *ALP*, *Runx2* and *OCN*, meanwhile 10 µM of LC exerts an opposite effect that promotes NIH3T3 osteogenesis. Mechanistically, 100 µM LC significantly inhibits IGF-1/PI3K/Akt signalling, while 10 µM LC slightly activates this pathway. Our study suggests that a decease in LC level might contribute to the development of ectopic calcification in fibroblasts by affecting IGF-1/PI3K/Akt, and addition of LC may benefit patients with ectopic calcification.**

Keywords: Ectopic calcification, fibroblast, L-carnitine, IGF-1/PI3K/Akt, proliferation, osteoblastic differentiation

1. Introduction

Ectopic calcification is defined as inappropriate deposition of calcium/phosphate complexes in connective tissues in aberrant locations (*1*). Pseudoxanthoma elasticum (PXE) is a prototype of multisystem ectopic mineralization disorders characterized by calcium phosphate deposition in various tissues (*2*). PXE is caused by mutations in the *ABCC6* gene which encodes for a putative transmembrane transporter protein, ABCC6 (*3-5*). The *Abcc6*^{-/-} mouse which recapitulates the features of PXE, is a mouse model of PXE including

extensive mineralization in the arterial blood vessels, skin and Bruch's membrane in the eyes (*6,7*). Fibroblasts are present in all connective tissues, which are the main component of dense connective tissue and the progenitors of ectopic calcification (*8*). Osteoblasts and fibroblasts are both of mesenchymal origin. In cell morphology, osteoblasts are nearly indistinguishable from fibroblasts, except for the formation of mineralized extracellular matrix which locates outside the cells. Additionally, all the genes expressed in fibroblasts are also expressed in osteoblasts, but osteoblasts express only two osteoblast-specific transcripts: one encoding runt-related transcription factor 2 (Runx2), a transcription factor, and the other encoding osteocalcin (OCN), a secreted molecule (*9*). Thus, fibroblasts and osteoblasts may express mutual transformation behavior due to the same origin, partial overlap of phenotype, and similarity of differentiation. Previous studies have indicated that fibroblasts can convert to osteoblasts and form bone

Address correspondence to:
Dr. Jinxiang Han, Key Laboratory for Rare Disease Research of Shandong Province, Key Laboratory for Biotech Drugs of the Ministry of Health, Shandong Medical Biotechnological Center, Shandong Academy of Medical Sciences, Ji'nan, Shandong 250062, China.
E-mail: jxhan9888@aliyun.com

in vitro through induction of inflammatory mediators, TGF-β, *etc*. (*10*). Furthermore, *in vivo* experiments also confirmed that when there was an appropriate stimulus condition (*e.g.* bone chips), fibroblasts became active, could be transformed into osteoblasts, and finally formed mineralized nodules (*11*).

Cellular metabolic activity plays an important role in regulating cell survival, differentiation and tissue growth (*12*). L-carnitine (LC) is a trimethylated amino acid which is an essential cofactor for the transport of long-chain fatty acids across the inner mitochondrial membrane into the mitochondrial matrix for their subsequent β-oxidation (*13*). LC facilitates energy availability, and is especially important for those tissues with high energy requirements. Studies indicated that cells of the osteoblastic lineage generate 40% to 80% of their energy demands through fatty acid β-oxidation (*14*). It has also been demonstrated that LC could protect osteoblastic cells from apoptosis (*15,16*), increased metabolic activity and protein production of porcine osteoblast-like cells (*17*), as well as affected osteoblastic activity (*15*).

Further studies *in vivo* and *in vitro* have suggested that proliferating and differentiating factors which affect osteoblastic activity exert their roles through the involvement of insulin-like growth factor (IGF) expression (*18*). IGF-1 is produced and stored in the bone matrix which stimulates proliferation and differentiation of osteoblasts (*19-21*). Moreover, studies in animals and humans have shown that supplementation with LC increased plasma concentrations of IGF-1 (*22-24*). IGF-1 plays an important role in the activation of the IGF-1/PI3K/Akt signaling pathway. Binding of IGF-1 to its receptor results in a multiple auto-phosphorylation cascade. As a consequence, phosphoinositide-3-kinase (PI3K) is activated, and then its downstream Akt translocates to the membrane, where it becomes phosphorylated (at threonine 308 and serine 473) and is thereby activated by PI3K (*25,26*). Considerable evidence collected *in vitro* and *in vivo* substantiated that the activation of the IGF-1/PI3K/Akt pathway could effectively increase osteoblast differentiation and calcification (*27,28*).

Our understanding of the effects of LC on osteoblastic differentiation and mineralization has been advanced by our previous study on the metabonomics analysis of *Abcc6*$^{-/-}$ knock-out mice whose LC concentration was decreased in plasma. Therefore, we hypothesized that LC may have a negative impact on osteoblastic differentiation and mineralization. To investigate this hypothesis, we performed an experiment with a cell model of ectopic calcification, cultured NIH3T3 cells in a Pi-inducing medium which allowed mineralization to occur. To elucidate the effects on osteoblast differentiation and mineralization *in vitro*, the results were evaluated on mineralized nodule formation, calcium deposits, ALP activity and expression of osteogenic marker genes.

2. Materials and Methods

2.1. *Cell culture and treatment*

Mouse embryonic fibroblast cells NIH 3T3 cells, obtained from the Cell Bank of Type Culture Collection of the Chinese Academy of Sciences (Shanghai, China), were routinely cultured in DMEM (Gibco, Carlsbad, CA, USA) normal growth medium supplemented with 10% (v/v) fetal bovine serum (Gibco, Carlsbad, CA, USA), 100 U/mL penicillin, and 100 μg/mL streptomycin (both from Invitrogen, Carlsbad, CA, USA). At about 80% confluence, cells were switched to Pi-inducing medium consisting of the normal growth medium described above supplemented with 2 mM Na$_3$PO$_4$ (*29*) which represented the control, or to Pi-inducing medium supplemented with 10 μM LC (Santa Cruz, California, USA) or 100 μM LC. Cells were then continued to be cultured at 37°C in a humidified atmosphere containing 5% (v/v) CO$_2$ for up to 7 days or 12 days. The medium was replaced every 2 days and the first day of culture in Pi-inducing medium was defined as day 0.

2.2. *Cell proliferation analysis*

Cell proliferations of NIH3T3 cells undergoing osteoblast differentiation with different LC concentrations were investigated by 3-[4, 5-dimethylthiazol-2-yl]-2, 5 diphenyl tetrazolium bromide (MTT) assay, which is a sensitive quantitative colorimetric assay (*30*). Cells were seeded on 96-well plates and treated for 24 h, 48 h and 72 h. The effects of LC on osteoblast proliferation were evaluated every 24 hours for 3 days. MTT reagent (5 mg/mL) was added to each well after the medium had been aspirated, and incubated for 4 h at 37°C , then formazan crystals were dissolved in dimethyl sulfoxide (DMSO) and the absorbance was measured at 490 nm using Bio-Tek Synergy HT.

2.3. *Mineralization analysis*

To measure mineralized nodule formation, the cellular matrix was stained using a special, calcium-specific stain, Alizarin Red S (AR-S) dye, which is an indicator of mineralization (*31*). NIH3T3 cells were seeded on 24-well plates and treated for 12 days, after that the cells were washed three times with phosphate-buffered saline (PBS) and fixed with 4% paraformaldehyde for 10 min, and then were stained with 0.5% (w/v) AR-S solution for 30 min at room temperature. Dye was thoroughly washed three times with PBS and the images of the stained cells were captured. For quantitative analyses of the mineralization indicated by AR-S, the cells were incubated in 10% (w/v) cetylpyridium chloride at 37°C for 1 h. The absorbance

of the supernatant was measured at 562 nm (*32*).

2.4. *Calcium deposition analysis*

NIH3T3 cells were seeded on 24-well plates, after 12 days of treatment the cells were decalcified with 0.6 mol/L HCl at 37°C for 24 h. The calcium content of the HCl supernatant was determined using a Calcium Assay Kit (Sigma, St. Louis, MO, USA) (*33*). After decalcification, cells were washed three times with PBS and solubilized with 0.1 mol/L NaOH/0.1% SDS at 4°C for 1 h. The protein content was measured with a BCA Protein Assay kit (Thermo Scientific, Rockford, IL, USA), and the calcium content of the cell layer was normalized by protein content.

2.5. *Alkaline phosphatase activity analysis*

LabAssay™ ALP kit (Wako, Osaka, Japan) was used to measure the expression of ALP. This kit uses p-nitrophenylphosphate as a substrate, and released p-nitrophenol measured at 405 nm as the enzyme activity. After 12 days of culture, NIH3T3 cells were lysed by addition of 200 μL buffer containing 25 mM Tris-HCl (pH 7.4) and 0.5% Triton X-100 (*34*), using three cycles of freezing and thawing to verify that the cells were completely lysed. Then, 20 μL of cell lysate was mixed with 100 μL working assay solution and incubated for 15 min at 37°C. The reaction was stopped by addition of 80 μL stop solution and the absorbance at 405 nm was measured by microplate reader. The ALP activity was normalized by the total protein concentration for each sample using the BCA method.

2.6. *RNA isolation and quantitative real-time polymerase chain reaction (RT-qPCR)*

RNA levels were analyzed by real-time PCR in cells treated for 7 days or 12 days. Total RNA was extracted from 24-well plates using Trizol reagent (Gibco, Carlsbad, CA, USA) and the purified total RNA was used for cDNA synthesis with a first-strand cDNA synthesis kit (Toyobo, Osaka, Japan). After the RT reaction, cDNA was used as the template for RT-qPCR of *Runx2*, *ALP*, *OCN* and *IGF-1*. Glyceraldehyde-3-phosphatedehydrogenase (*GAPDH*) served as the internal control. RT-qPCR was performed using a SYBR Green qPCR Kit (Toyobo, Osaka, Japan) in a real-time PCR detection system, LightCycler 480 thermocycler (Roche Applied Science, Mannheim, Germany) with gene-specific primers: 5'-TGG CTC TGC CTT TAT TCC CTA GT-3' and 5'-AAA TAA GGT GCT TTG GGA ATC TGT-3' for *ALP*, 5'-AAG TGC GGT GCA AAC TTT CT-3' and 5'-TCT CGG TGG CTG GTA GTG A-3' for *Runx2*, 5'-TGC TTG TGA CGA GCT ATC AG-3' and 5'-GAG GAC AGG GAG GAT CAA GT-3' for *OCN*, 5'-GCT CTG CTT GCT CAC CTT C-3'

and 5'-TCA GTG GGG CAC AGT ACA TC-3' for *IGF-1* and 5'-ACC ACA GTC CAT GCC ATC AC-3' and 5'-TCC ACC ACC CTG TTG CTG TA-3' for *GAPDH*. The transcript levels were normalized using the *GAPDH* transcript levels.

2.7. *Western blotting*

NIH3T3 cells were collected after 7 days of treatment, and the cells were homogenized in cell lysis buffer for Western and IP (Beyotime, Shanghai, China) supplemented with protease and phosphatase inhibitors on ice for 60 min and centrifuged at 13,000 g for 15 min at 4°C. Total protein concentration of the cell lysate was determined by the BCA method. Forty micrograms of the total protein from each sample was suspended in Laemmli loading buffer and incubated at 95°C for 5 min. Proteins were separated using 12% sodium dodecyl sulfate polyacrylamide gel electrophoresis (SDS-PAGE) gels and transferred to a polyvinylidene fluoride (PVDF) membrane. After 1 h of blocking with 5% low fat milk in TBST (10 mM Tris, 100 mM NaCl, and 0.05% Tween-20), membranes were incubated overnight at 4°C with the specific antibodies for goat polyclonal anti-mouse Runx2 (C-19) (1:500) (Santa Cruz Biotechnology, Carlsbad, CA, USA), rabbit polyclonal anti-mouse Akt (1:1,000) (Cell Signaling Technology, Danvers, MA, USA), rabbit monoclonal anti-mouse Phospho-Akt (Ser473) (1:2000) (Cell Signaling Technology, Danvers, MA, USA), and mouse monoclonal anti-mouse GAPDH (G-9) (1:1,000) (Santa Cruz Biotechnology, Carlsbad, CA, USA). Primary antibodies were immunostained with the appropriate peroxidase-conjugated secondary antibodies. Finally, the blots were developed with enhanced chemiluminescence (ECL) (Millipore Corporation, Billerica, MA, USA) and exposed to X-ray film.

2.9. *Statistical analysis*

Statistical analyses were performed using SPSS-17.0 software (SPSS Inc., Chicago, IL, USA). Results are expressed as the mean ± S.D. All data were analyzed by analysis of variance (ANOVA) and unpaired Student's *t*-test. Statistical significance between groups was defined as $p < 0.05$.

3. Results

3.1. *Effects of LC on the proliferation of NIH3T3 cells*

MTT assay is a main application that allows for proliferation of cells to be assessed. The absorbance of each well at 490 nm was measured after treatment for 24, 48 and 72 h. To compare with the control group, no significant differences were observed between them at 24 and 48 h, but after 72 h, the Absorbance values of the

10 μM LC group were slightly higher, while the 100 μM LC group were slightly reduced (Figure 1). Therefore, the MTT assay indicated that 10 μM LC increased the proliferation of NIH3T3 cells, but 100 μM LC slightly inhibited cell proliferation.

3.2. *Effects of LC on the osteogenic activities in NIH3T3 cells*

First, we investigated whether ALP activity was altered during LC treatment in NIH3T3 cells. In this study, we found that the ALP activity in the 10 μM LC group was much higher, but in the 100 μM LC group was lower than the control group ($p < 0.05$, Figure 2A). Therefore, this indicates that 10 μM LC can promote ALP activity, while 100 μM LC suppresses the ALP activity in NIH3T3 cells. Next, the expression of Runx2 was determined by Western blotting analysis. The result showed that the expression of Runx2 was upregulated in 10 μM LC treated cells and was markedly dowregulated in 100 μM LC treated cells compared with the control cells at 7 days (Figure 2B). Together, these results suggest that LC has alterable effects on the osteogenic activities in NIH3T3 cells; either increased or decreased depending on the levels of specific concentration. Low concentration of LC facilitates osteoblast differentiation, while high concentration of LC counteracts the process in NIH3T3 cells.

3.3. *Effects of LC on the mineralization in NIH3T3 cells*

In this study, we confirmed the mineralization of NIH3T3 cells by AR-S stain. As shown in Figure 3A, obvious mineralized nodules were noted in 10 μM LC, but decreased in 100 μM LC in comparison to the control. To evaluate calcium deposition in the NIH3T3 cell matrix, quantitative assays of mineralization were carried out after incubation in cetylpyridium chloride. The results revealed that calcium deposition under the 10 μM LC condition was increased, whereas the 100 μM LC condition was decreased ($p < 0.05$, Figure 3B). To further examine the mineralization, the calcium depositions were also carried out using a Calcium Assay Kit. The data were consistent with the AR-S stain ($p < 0.05$, Figure 3C). These results provided further evidence that 10 μM LC had a positive effect on osteoblast differentiation and mineralization in NIH3T3 cells, whereas 100 μM LC had an opposite effect.

3.4. *Effects of LC on the expression of osteogenic marker genes in NIH3T3 cells*

To gain further insight into the molecular mechanism of LC function in osteoblast differentiation, the expression of typical osteogenic marker genes (*Runx2*, *ALP*, and *OCN*) were examined by realtime PCR. The expression level of *Runx2*, which regulates osteoblast
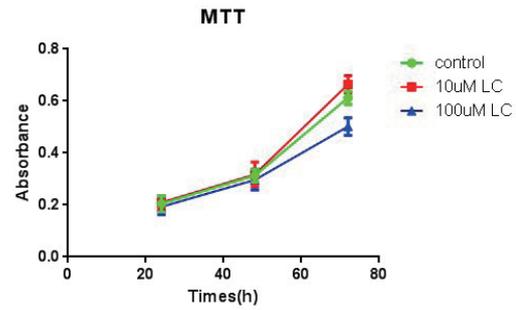

Figure 1. Effects of LC on the proliferation of NIH3T3 cells. The proliferation of NIH3T3 cells was measured by MTT assays after treatment with 10 or 100 μM LC or no treatment (control) for 24 h, 48 h and 72 h. Data are expressed as the mean ± S.D., $n = 6$. $^*p < 0.05$, *vs.* control.
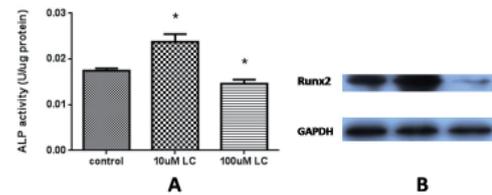

Figure 2. Effects of LC on osteogenic activities in NIH3T3 cells. The ALP activity (A) and Runx2 expression (B) were determined by LabAssay™ ALP kit and Western blotting analysis, respectively. NIH3T3 cells induced with Pi-inducing medium after treatment with 10 or 100 μM LC or no treatment (control) for 7 or 12 days are shown. Bars are shown as the mean ± S.D., $n = 3$. $^*p < 0.05$ *vs.* control.
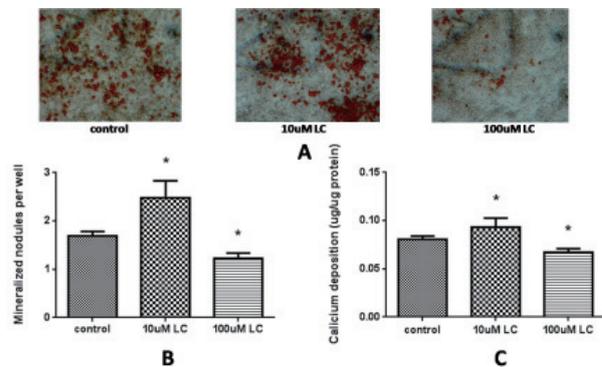

Figure 3. Effects of LC on matrix mineralization in NIH3T3 cells. The calcium deposits in the mineralized matrix were analyzed by Alizarin Red S staining **(A)** which was quantified at 562 nm **(B)** and Calcium Assay Kit **(C)**. NIH3T3 cells induced with Pi-inducing medium after treatment with 10 or 100 μM LC or no treatment (control) for 12 days are shown. Bars are shown as the mean ± S.D., $n = 3$. $^*p < 0.05$, *vs.* control.

differentiation at the early stages, was markedly upregulated in the 10 μM LC group, and downregulated in the 100 μM LC group compared with the control at 7 days (Figure 4A). The expressions of *ALP* and *OCN* in the 10 μM LC group and 100 μM LC group were significantly higher or lower than the control group at 12 days (Figures 4B and 4C). These results also suggest that 10 μM LC can facilitate osteoblast differentiation, while 100 μM LC inhibits osteoblast differentiation in NIH3T3 cells which is consistent with mineralized
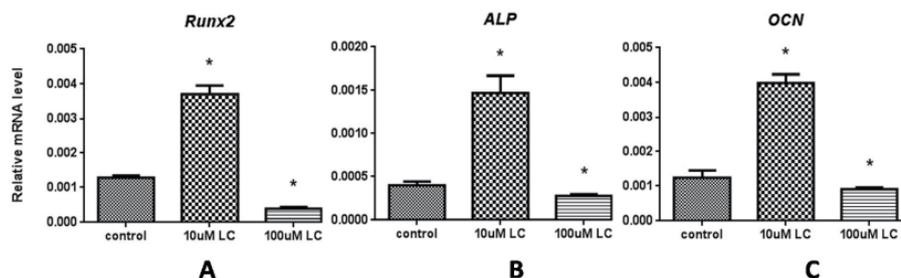
Figure 4. Effects of LC on expression levels of different osteoblast differentiation marker genes in NIH3T3 cells. Real-time PCR analyses of the *Runx2* **(A)**, *ALP* **(B)**, and *OCN* **(C)** mRNA levels in NIH3T3 cells induced with Pi-inducing medium after treatment with 10 or 100 μM LC or no treatment (control) for 7 or 12 days are shown. The results were normalized by the mRNA levels of *GAPDH* as a housekeeping gene. Results are the mean ± S.D., *n* = 3. * *p* < 0.05 *vs.* control.
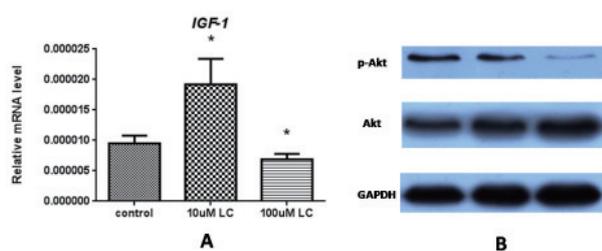

Figure 5. Effects of LC on the IGF-1/PI3K/Akt signaling pathway in NIH3T3 cells. Real-time PCR analyses of *IGF-1***(A)** and Western blotting analysis of p-Akt and Akt proteins **(B)** in NIH3T3 cells induced with Pi-inducing medium after treatment with 10 or 100 μM LC or no treatment (control) for 7 days are shown. Data are expressed as the mean ± S.D., *n* = 3. * *p* < 0.05, *vs.* control.

nodule formation, calcium deposition, ALP activity and the expression of Runx2 shown above.

3.5. *Effects of LC on the IGF-1/PI3K/Akt signaling pathway in NIH3T3 cells*

In order to investigate whether LC could have an influence on the IGF-1/PI3K/Akt signaling pathway, we used RT-PCR and Western blot analysis. RT-PCR showed that the mRNA expression of *IGF-1*, was upregulated in the 10 μM LC group, and downregulated in the 100 μM LC group compared with the control at 7 days (Figure 5A). This demonstrated that 10 μM LC increases expression of *IGF-1*, but 100 μM LC decreases expression. Moreover, we identified the protein expression of Phospho-Akt (p-Akt) by Western blot analysis after 7 days treatment. As shown in Figure 5B, although the expression level of p-Akt protein had no significant difference when treated with 10 μM LC, the 100 μM LC was significantly lower than the control at 7 days. As well as the total mass of Akt protein had no significant difference between the three groups. This suggested that supplementation of 100 μM LC leads to an inactivation of the IGF-1/PI3K/Akt signalling pathway.

4. Discussion

Ectopic calcification is a common problem associated

with several clinical conditions, such as aging, organ injury, and autoimmune diseases. Studies have noted that several factors, either systemic or local, can antagonize the aberrant mineralization of connective tissues (*35*). In spite of the fact that molecular mechanisms underlying the regulation of ectopic calcification are unclear, some evidence has emerged in support of the concept that ectopic calcification is a cell regulated process (*36*). To test the possible roles of LC in ectopic mineralization, we cultured NIH3T3 cells in Pi-inducing medium and supplemented with LC. Cells undergo a phenotypic transition into osteoblast cells, evidenced by an increase in mineralized nodule formation and calcium deposits.

During the early stage of osteoblast differentiation, osteoblasts synthesize Runx2, ALP and other osteoblastic differentiation markers, ultimately leading to the induction of extracellular matrix calcification (*37,38*). Runx2 is a crucial transcription factor which regulates the expression of major bone matrix protein genes and determines osteoblast differentiation (*39*). Runx2 has been shown to regulate the expression of OCN (*40*). OCN is essential for hydroxyapatite binding and deposition in the extracellular matrix of bone, whose synthetic peak is consistent with the peak of ALP activity (*41*). ALP is a well-established phenotypic marker of osteoblast differentiation and a critical enzyme in calcification (*42*). In this study, we found that both the mRNA and protein levels of Runx2 were increased in the 100 μM LC group and decreased in the 10 μM LC group compared with the control. It demonstrated that LC could affect the differentiation of osteoblasts by regulating the level of Runx2 expression. The results were parallel to the gene expression of *ALP*, *OCN* and ALP activity. Most importantly, the formation of mineralized nodules in NIH3T3 cells evaluated by AR-S and calcium deposits provided powerful evidence. Taken together, these results suggest that LC exerted a dominant effect on osteoblast differentiation and mineralization in NIH3T3 cells.

Some studies suggest that LC promoted osteoblast proliferation and differentiation *in vitro* (*43,44*), while other studies indicated that LC inhibited proliferation in VSMCs (*45*). In this study, we found that the 10 μM LC positively affected osteoblast proliferation,

but the higher concentration of LC (100 μM) slightly decreased osteoblast proliferation compared with the control. Meanwhile, it has recently been demonstrated that supplementation of LC lead to an activation of the IGF-1/PI3K/Akt signalling pathway (*46*). Therefore, we investigated whether the effect of LC on proliferation and osteoblast differentiation could be mediated by the IGF-1/PI3K/Akt signalling pathway. To this end, we tested the effects of LC on *IGF-1*, p-Akt and Akt expression by RT-qPCR and Western blot analysis. The results showed that the gene expression of *IGF-1* and the protein level of p-Akt were downregulated in the 100 μM LC treated cells. Consequently, we postulate that the proliferation and osteoblast differentiation effects on fibroblasts could be in turn responsible for the IGF-1/PI3K/Akt signalling pathway induced by LC. Taking all the experiments together, our study indicates that the higher concentration of LC (100 μM) slightly inhibits osteoblast proliferation, and plays negative roles in osteoblast differentiation and mineralized bone matrix formation in fibroblast cells, which is consistent with our previous study on the metabonomics analysis of $Abcc6^{-/-}$ knock-out mice whose LC concentration was decreased in plasma.

In conclusion, our data have demonstrated for the first time that supplementation of 100 μM LC leads to an inactivation of the IGF-1/PI3K/Akt signalling pathway, and slightly inhibits the proliferation and osteoblast differentiation of fibroblast cells. So far there is no effective treatment for the systemic manifestations of ectopic mineralization disorders. From this point of view, we have probably provided a reasonable basis for the potential utility of LC in the prevention and treatment of ectopic calcification, although gaining a better understanding of the mechanism should lead to improved prevention and treatment of ectopic calcification in the future. In a follow-up study, we will continue to study the mechanism underlying ectopic calcification prevention and treatment by LC.

Acknowledgements

References

1. Cotran RS, Kumare V, Robbins SL. Cellular injury and cellular death. In: Pathological Basis of Disease. 5th ed., WB Saunders Press, Philadelphia, PA, USA, 1994; pp. 1-35.
2. Uitto J, Li Q, Jiang Q. Pseudoxanthoma elasticum: Molecular genetics and putative pathomechanisms. J Invest Dermatol. 2010; 130:66.
3. Ringpfeil F, Lebwohl MG, Christiano AM, Uitto J. Pseudoxanthoma elasticum: Mutations in the *MRP6* gene encoding a transmembrane ATP-binding cassette (ABC) transporter. Proc Natl Acad Sci U S A. 2000; 97:6001-6006.
4. Le Saux O, Urban Z, Tschuch C, Csiszar K, Bacchelli B, Quaglino D, Pasquali-Ronchetti I, Pope FM, Richards A, Terry S, Bercovitch L, de Paepe A, Boyd CD. Mutations in a gene encoding an ABC transporter cause pseudoxanthoma elasticum. Nat Genet. 2000; 25:223-227.
5. Bergen AA, Plomp AS, Schuurman EJ, Terry S, Breuning M, Dauwerse H, Swart J, Kool M, van Soest S, Baas F, ten Brink JB, de Jong PT. Mutations in *ABCC6* cause pseudoxanthoma elasticum. Nat Genet. 2000; 25:228-231.
6. Gorgels TG, Hu X, Scheffer GL, van der Wal AC, Toonstra J, de Jong PT, van Kuppevelt TH, Levelt CN, de Wolf A, Loves WJ, Scheper RJ, Peek R, Bergen AA. Disruption of *Abcc6* in the mouse: Novel insight in the pathogenesis of pseudoxanthoma elasticum. Hum Mol Genet. 2005; 14:1763-1773.
7. Klement JF, Matsuzaki Y, Jiang QJ, Terlizzi J, Choi HY, Fujimoto N, Li K, Pulkkinen L, Birk DE, Sundberg JP, Uitto J. Targeted ablation of the *Abcc6* gene results in ectopic mineralization of connective tissues. Mol Cell Biol. 2005; 25:8299-8310.
8. Friedenstein AY. Induction of bone tissue by transitional epithelium. Clin Orthop Relat Res. 1968; 59:21-37.
9. Ducy P, Schinke T, Karsenty G. The osteoblast: A sophisticated fibroblast under central surveillance. Science. 2000; 289:1501-1504.
10. Rutherford RB, Moalli M, Franceschi RT, Wang D, Gu K, Krebsbach PH. Bone morphogenetic protein-transduced human fibroblasts convert to osteoblasts and form bone *in vivo*. Tissue Eng. 2002; 8:441-52.
11. Reddi AH, Huggins C. Biochemical sequences in the transformation of normal fibroblasts in adolescent rats. Proc Natl Acad Sci U S A. 1972; 69:1601-1605.
12. Zhang J, Khvorostov I, Hong JS, *et al*. UCP2 regulates energy metabolism and differentiation potential of human pluripotent stem cells. EMBO J. 2011; 30: 4860-4873.
13. Borum PR. Regulation of carnitine concentration in plasma. In: Carnitine biosynthesis, metabolism and functions (Frenkel RA, McGarry JD, eds.). Academic Press, New York, USA, 1980; pp. 115-126.
14. Adamek G, Felix R, Guenther HL, Fleisch H. Fatty acid oxidation in bone tissue and bone cells in culture. Biochem J. 1987; 242:129-137.
15. Colucci S, Mori G, Vaira S, Brunetti G, Greco G, Mancini L, Simone GM, Sardelli F, Koverech A, Zallone A, Grano M. L-Carnitine and isovaleryl L-carnitine fumarate positively affect human osteoblast proliferation and differentiation *in vitro*. Calcif Tissue Int. 2005; 6:458-465.
16. Xie H, Tang SY, Li H, Luo XH, Yuan LQ, Wang D, Liao EY. L-Carnitine protects against apoptosis of murine MC3T3-E1 osteoblastic cells. Amino Acids. 2008; 2:419-423.
17. Chiu KM, Keller ET, Crenshaw TD, Gravenstein S. Carnitine and dehydroepiandrosterone sulphate induced protein synthesis in porcine osteoblast-like cells. Calcif Tissue Int. 1999; 64:527-533.
18. Mohan S, Baylink DJ. Insulin-like growth factor system components and the coupling of bone formation to

resorption. Horm Res. 1996; 45(Suppl 1):59-62.

19. Jonsson KB, Ljunghall S, Karlström O, Johansson AG, Mallmin H, Ljunggren O. Insulin-like growth factor I enhances the formation of type I collagen in hydrocortisone-treated human. Biosci Rep. 1993; 13:297-302.

20. Gangji V, Rydziel S, Gabbitas B, Canalis E. Insulin-like growth factor II promoter expression in cultured rodent osteoblasts and adult rat bone. Endocrinology. 1998; 139:2287-2292.

21. Langdahl BL, Kassem M, Møller MK, Eriksen EF. The effects of IGF-I and IGF-II on proliferation and differentiation of human osteoblasts and interactions with growth hormone. Eur J Clin Invest. 1998; 28:176-183.

22. Heo YR, Kang CW, Cha YS. L-Carnitine changes the levels of insulin-like growth factors (IGFs) and IGF binding proteins in streptozotocin-induced diabetic rat. J Nutr Sci Vitaminol (Tokyo). 2001; 47:329-334.

23. Kita K, Kato S, Amanyaman M, Okumura J, Yokota H. Dietary L-carnitine increases plasma insulin-like growth factor-I concentration in chicks fed a diet with adequate dietary protein level. Br Poult Sci. 2002; 43:117-121.

24. Doberenz J, Birkenfeld C, Kluge H, Eder K. Effects of L-carnitine supplementation in pregnant sows on plasma concentrations of insulin-like growth factors, various hormones and metabolites and chorion characteristics. J Anim Physiol Anim Nutr (Berl). 2006; 90:487-499.

25. Cantley LC. The phosphoinositide 3-kinase pathway. Science. 2002; 296:1655-1657.

26. Hofler A, Nichols T, Grant S, Lingardo L, Esposito EA, Gridley S, Murphy ST, Kath JC, Cronin CN, Kraus M, Alton G, Xie Z, Sutton S, Gehring M, Ermolieff J. Study of the PDK1/AKT signaling pathway using selective PDK1 inhibitors, HCS, and enhanced biochemical assays. Anal Biochem. 2011; 414:179-186.

27. Chen LL, Huang M, Tan JY, Chen XT, Lei LH, Wu YM, Zhang DY. PI3K/AKT pathway involvement in the osteogenic effects of osteoclast culture supernatants on preosteoblast cells. Tissue Eng Part A. 2013; 19:2226-2232.

28. Suzuki E, Ochiai-Shino H, Aoki H, Onodera S, Saito A, Saito A, Azuma T. Akt activation is required for TGF-β1-Induced osteoblast differentiation of MC3T3-E1 pre-osteoblasts. PLoS One. 2014; 9:e112566.

29. Jono S, McKee MD, Murry CE, Shioi A, Nishizawa Y, Morii H, Giachelli CM. Phosphate regulation of vascular smooth muscle cell calcification. Circ Res. 2000; 87:e10-17.

30. Castiglioni S, Casati S, Ottria R, Ciuffredav P, Maier JA. N6-isopentenyladenosine and its analogue N6-benzyladenosine induce cell cycle arrest and apoptosis in bladder carcinoma T24 cells. Anticancer Agents Med Chem. 2013; 13:672-678.

31. Yamakawa K, Iwasaki H, Masuda I, Ohjimi Y, Honda I, Saeki K, Zhang J, Shono E, Natio M, Kikuchi M. The utility alizarin red s staining in calcium pyrophosphate dihydrate crystal deposition disease. J Rheumatol. 2003; 30: 1032-1035.

32. Stanford CM, Jacobson PA, Eanes ED, Lembke LA, Midura RJ. Rapidly forming apatitic mineral in an osteoblastic cell line (UMR 106-01 BSP). J Biol Chem.

1995; 270:9420-9428.

33. Hernandez L, Park KH, Cai SQ, Qin L, Partridge N, Sesti F. The antiproliferative role of ERG K+ channels in rat osteoblastic cells. Cell Biochem Biophys. 2007; 47:199-208.

34. Zhang YY, Cui YZ, Luan J, Zhou XY, Zhang GL, Han JX. Platelet-derived growth factor receptor kinase inhibitor AG-1295 promotes osteoblast differentiation in MC3T3-E1 cells via the Erk pathway. Biosci Trends. 2012; 6:130-135.

35. Rutsch F, Nitschke Y, Terkeltaub R. Genetics in arterial calcification: Pieces of a puzzle and cogs in a wheel. Circ Res. 2011; 109:578-592.

36. Giachelli CM. Ectopic calcification: Gathering hard facts about soft tissue mineralization. Am J Pathol. 1999; 154:671-675.

37. Beresford JN, Graves SE, Smoothy CA. Formation of mineralized nodules by bone derived cells *in vitro*: A model of bone formation? Am J Med Genet. 1993; 45:163-178.

38. Stein GS, Lian JB, Owen TA. Relationship of cell growth to the regulation of tissue-specific gene expression during osteoblast differentiation. FASEB J. 1990; 4:3111-3123.

39. Ji C, Casinghino S, Chang DJ, Chen Y, Javed A, Ito Y, Hiebert SW, Lian JB, Stein GS, McCarthy TL, Centrella M. CBFa(AML/PEBP2)-related elements in the TGF-beta type I receptor promoter and expression with osteoblast differentiation. J Cell Biochem. 1998; 69:353-363.

40. Komori T. Regulation of bone development and extracellular matrix protein genes by RUNX2. Cell Tissue Res. 2010; 339:189-195.

41. Patti A, Gennari L, Merlotti D, Dotta F, Nuti R. Endocrine actions of osteocalcin. Int J Endocrinol. 2013; 2013:846480.

42. Weinreb M, Shinar D, Rodan GA. Different pattern of alkaline phosphatase, osteopontin, and osteocalcin expression in developing rat bone visualized by in situ hybridization. J Bone Miner Res. 1990; 5:831-842.

43. Keller J, Couturier A, Haferkamp M, Most E, Eder K. Supplementation of carnitine leads to an activation of the IGF-1/PI3K/Akt signaling pathway and down regulates the E3 ligase MuRF1 in skeletal muscle of rats. Nutr Metab (Lond). 2013; 10:28.

44. Colucci S, Mori G, Vaira S, Brunetti G, Greco G, Mancini L, Simone GM, Sardelli F, Koverech A, Zallone A, Grano M. L-carnitine and isovaleryl L-carnitine fumarate positively affect human osteoblast proliferation and differentiation of adult stem cells. Calcif Tissue Int. 2005; 76:458-465.

45. Lu Q, Zhang Y, Elisseef JH. Carnitine and accetylcarnitine modulate mesenchymal differentiation of adult stem cells. J Tissue Eng Regen Med. 2013; 1747. (doi: 10.1002/term.1747)

46. Xie H, Yang B, Zhou XM, Song FL, Li JM, Zhou K, Hu W, Peng YQ, Tang SY, Yuan LQ, Xiong SY, Liao XB. L-carnitine and taurine synergistically inhibit the proliferation and osteoblastic differentiation of vascular smooth muscle cells. Acta Pharmacol Sin. 2010; 31:289-296.